Agricultural Water Management 263 (2022) 107491

Contents lists available at ScienceDirect

Agricultural Water Management

journal homepage: www.elsevier.com/locate/agwat

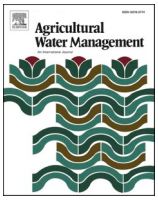

Calibration and validation of the FAO AquaCrop water productivity model for cassava (*Manihot esculenta* Crantz)

Joost Wellens [a,b,*], Dirk Raes [c], Elias Fereres [d,e], Jan Diels [c], Cecilia Coppye [c], Joy Geraldine Adiele [f], Kodjovi Senam Guillaume Ezui [g,h], Luis-Augusto Becerra [i], Michael Gomez Selvaraj [i], Gerd Dercon [j], Lee Kheng Heng [k]

[a] University of Liège, TERRA Teaching and Research Centre, Gembloux Agro-Bio Tech, Passage des Déportés 2, 5030 Gembloux, Belgium
[b] University of Liège, SPHERES Research Unit, Arlon Campus Environnement, Avenue de Longwy 185, 6700 Arlon, Belgium
[c] KU Leuven University, Department of Earth and Environmental Sciences, Celestijnenlaan 200 E, 3001 Leuven, Belgium
[d] Institute for Sustainable Agriculture, CSIC, Apartado 4084, 14080 Córdoba, Spain
[e] University of Cordoba, Department of Agronomy, Campus Rabanales C5, 14014 Córdoba, Spain
[f] National Root Crops Research Institute, Umudike, KM 8 Ikot Ekpene Road, P.O. Box 7006, Abia Sate, Nigeria
[g] African Plant Nutrition Institute (APNI), ICIPE Campus, Duduville – Kasarani, Thika Road, P.O. Box 30772-00100, Nairobi, Kenya
[h] International Fertilizer Development Centre (IFDC), ICIPE Campus, Duduville – Kasarani, Thika Road, P.O. Box 30772-00100, Nairobi, Kenya
[i] International Center for Tropical Agriculture (CIAT), A.A. 6713, Cali, Colombia
[j] Joint FAO/IAEA Centre of Nuclear Techniques in Food and Agriculture, Soil and Water Management & Crop Nutrition Laboratory, 2444 Seibersdorf, Austria
[k] Joint FAO/IAEA Centre of Nuclear Techniques in Food and Agriculture, Soil and Water Management & Crop Nutrition Section, 1400 Vienna, Austria

ARTICLE INFO

Handling Editor - Dr R. Thompson

Keywords:
Crop model
West-Africa
South-America
Canopy cover
Biomass
Yield

ABSTRACT

FAO's water-driven crop growth simulation model, AquaCrop, was calibrated and validated for cassava (*Manihot esculenta* Crantz). Existing datasets, used in similar published works, were shared covering several years and regions (Colombia, Nigeria and Togo). Different varieties were tested for the case of Colombia and a single variety (TME-419) for Nigeria and Togo. Overall calibrated biomass simulations resulted in an R^2 of 0.96 and a RMSE of 1.99 tonne DM/ha. As for dry tuber yield estimates, it was not possible to find a single harvest index for the ensembled varieties given their varying characteristics and limited data per variety. However, for the TME-419 variety (Nigeria and Togo) calibrated root tuber simulations yielded and R^2 of 0.94 and a RMSE of 2.37 tonne DM/ha. A single crop-file was developed for different cassava varieties and agro-ecological regions, which can be applied with confidence to further study cassava related food security, water productivity, improved agronomic practices, etc.

1. Introduction

Cassava (*Manihot esculenta* Crantz) is the primary food source for more than 800 million people, making it the 6th most important crop globally after wheat, rice, corn, potato and barley (Lebot, 2008) and the 4th most important crop commodity in Africa (López-Lavalle et al., 2021). The global production is estimated at around 300 million tonnes. Globally, about 63% of cassava is produced in Africa, 28% in Asia and 9% in the Americas. Nigeria is the largest cassava producing country in the world with about 60 million tonnes fresh storage root yield; Togo is ranked 30th on a list of 98 cassava producing countries with about 1 million tonnes. Paraguay is the highest ranked South-American cassava producing country at 20th position on the list with about 3.5 million tonnes; Colombia ranks 32nd producing about 1 million tonnes of fresh storage root yield (FAOSTAT, 2021).

As numerous communities' food security and livelihoods are dependent on cassava, and, with production increasing to keep pace with the increasing population, prediction of both the effects of the environment and of agronomic management on cassava production has become crucial. In addition to the growing population, many regions and communities around the world are facing or will face water scarcity due to anthropogenic pressures and climate crisis. There is a growing

* Corresponding author at: University of Liège, TERRA Teaching and Research Centre, Gembloux Agro-Bio Tech, Passage des Déportés 2, 5030 Gembloux, Belgium.
E-mail addresses: joost.wellens@uliege.be (J. Wellens), dirk.raes@kuleuven.be (D. Raes), ag1fecae@uco.es (E. Fereres), jan.diels@kuleuven.be (J. Diels), cecilia.coppye@live.be (C. Coppye), joyadiele@yahoo.com (J.G. Adiele), g.ezui@apni.net (K.S.G. Ezui), l.a.becerra@cgiar.org (L.-A. Becerra), m.selvaraj@cgiar.org (M.G. Selvaraj), G.Dercon@iaea.org (G. Dercon), L.Heng@iaea.org (L.K. Heng).

https://doi.org/10.1016/j.agwat.2022.107491
Received 12 August 2021; Received in revised form 12 January 2022; Accepted 13 January 2022
Available online 20 January 2022

uncertainty regarding water availability for agriculture. Agriculture uses as high as 70% of global fresh water withdrawals making it the biggest consumer of water. In this context, FAO developed the AquaCrop simulation model to help consultants, irrigation engineers, agronomists, (non-)governmental organizations and even farm managers with the formulation and evaluation of guidelines to increase crop water productivity with improved agronomic practices (Raes et al., 2009). This water-driven crop model simulates the evolution of attainable crop biomass and harvestable yield based on soil water content in the root zone. To facilitate the ease-of-use, the AquaCrop model only needs a relatively small number of parameters and mostly intuitive input variables (Steduto et al., 2009). With the release of several versions of the model, the calibration and validation of 15 important crops, amongst others, maize, wheat, rice, soybean, cotton, etc., was included (Steduto et al., 2012). New crops and studies are continuously being added by a constantly enlarging AquaCrop users' community: for crops such as cabbage (Kiptum et al., 2013; Wellens et al., 2013), for irrigation strategies (Geerts et al., 2010) or for simulations in batch-mode to make regional field level maize yield estimates (Abdoul-Hamid et al., 2019). However, cassava is a major crop which has not yet been calibrated and validated for AquaCrop.

Some well-known models have already been adapted successfully for cassava: the MANIHOT model, integrated in the DSSAT ('Decision Support System for Agrotechnology Transfer') package (Hoogenboom et al., 2018; Kumsueb and Jintrawet, 2020) and the LINTUL-cassava ('Light Interception and Utilization') model (Ezui et al., 2018; Adiele et al., 2021). In this present study, some of the cassava datasets used in the development and improvement of these models were shared to also calibrate and validate AquaCrop. These data are again briefly presented as part of this study; for more detailed information the reader is guided to the relevant references. The focus of this publication is on AquaCrop cassava model structure, the calibration and validation procedures, the results of the simulation, and the resulting cassava crop parameters file for AquaCrop.

2. Materials and methods

2.1. Description of AquaCrop model

FAO developed and freely distributes the AquaCrop model (Steduto et al., 2009). This dynamic crop growth model predicts biomass and yield response to water. FAO chose a water-driven growth engine since water is a crucial driver in agricultural production and often the limiting factor in attaining high yields. Another advantage of this water-driven approach is the fine balance between its robustness, accuracy and simplicity in formalization and parametrization (Geerts, 2008; Steduto et. al, 2009; Steduto et al., 2012). Actual crop transpiration (Tr) is translated into biomass (B) through a crop specific water productivity (WP) parameter (Eq. (1)) (Steduto, 2003). The WP exhibits a conservative behaviour when it is normalised (WP*) for evaporative demand and for CO_2 concentration (Steduto et al., 2007). The harvestable yield (Y) is portioned from the biomass by means of another crop (or variety) specific parameter defined as the harvest index (HI) (Eq. (2)).

$$B = WP \bullet \Sigma Tr \quad (1)$$

$$Y = HI \bullet B \quad (2)$$

Furthermore, the leaf area index (LAI), the usual indicator of canopy size in other crop models, has been replaced by the more straightforward fractional green canopy cover (CC: fractional coverage of green cover per unit of soil) to modulate crop transpiration and as a consequence biomass production. Crop responses to water stress are taken into account by means of an inclusive set of crop stress parameters (Ks; ranging from no stress 1 to full stress 0). Water stress may alter CC development by influencing leaf expansion (Ks_{exp}), canopy decline (Ks_{sen}) and maximum canopy cover. Water stress can also negatively impact transpiration through stomatal closure (Ks_{sto}), while water logging also affects transpiration (Ks_{aer}). A complete description of the concepts, underlying principles, algorithms and manuals are provided by Steduto et al. (2009, 2012), Raes et al. (2009) and Raes (2017a, 2017b).

Calibration and validation guidelines outlined by Steduto et al. (2012) were followed to parameterize a single cassava crop file which would be valid for the complete dataset used here. Initial calibration trials were carried out on the well-watered fields, free of any water stress (Table 1). In the first step, by comparing observed and simulated CC time series, the most important canopy characteristics were derived: days to emergence and maturity, canopy growth coefficient (CGC), maximum canopy cover (CCmax) and canopy decline coefficient (CDC). In the next step, the transpiration coefficient ($K_{c,Tr}$), the normalized water productivity (WP*), and the harvest index (HI) were modified to minimize the differences between observed and simulated biomass and final yield. WP* and $K_{c,Tr}$ were calibrated by plotting biomass against the transpiration sums normalized for ETo (Σ(Tr/ETo)), as proposed by Steduto et al. (2012). Biomass was normalized for CO_2. This consisted in considering the change of WP with the change of yearly CO_2 concentration (Steduto et al., 2007; 2012). Finally, by adding also the water limited datasets, the different water stress related parameters (Ks_{exp}, Ks_{sen}, Ks_{sto} and Ks_{aer}) were fine-tuned to further optimize simulation results.

Two thirds of the field data were used for calibration and the remaining for validation (Table 1). Quality of the calibration and validation procedure was assessed by means of statistical indicators Coefficient of Determination (R^2), Root Mean Square Error (RMSE), Normalized Root Mean Square Error (nRMSE) and Relative Root Mean Square Error (rRMSE) between observed and simulated final dry biomass and yield weight. This wider range of metrics was used for comparison with other published cassava simulations. Canopy cover simulations are considered an intermediate result and are evaluated visually. The current version of AquaCrop model (version 6.1) can only simulate yield formation of herbaceous crops with a single growing cycle (Raes, 2017b); so, all simulations were stopped after one cycle, coinciding with the drought induced dormancy period (see season lengths in Table 1).

2.2. Field data

Three datasets were made available for calibration and validation of the AquaCrop model (Table 1): i) a dataset retrieved from the DSSAT model (Hoogenboom et al., 2018) based on experiments performed by Veltkamp (1985) at the 'International Center for Tropical Agriculture' (CIAT) in Colombia; ii) a dataset received from the 'International Fertilizer Development Centre' (IFDC) in Togo documented by Ezui (2017) and Ezui et al. (2018); and iii) a third dataset provided by the 'African Cassava Agronomy Initiative' (ACAI) project of the 'International Institute of Tropical Agriculture' (IITA) in Nigeria and detailed in Adiele et al. (2021).

2.2.1. Climate data

Climate data for the weather station located in Palmira, Columbia (3.5380°N; 76.2972°W; 965 msl) were retrieved from DSSAT. Daily measured values were: minimum and maximum temperature, rainfall and solar radiation. DSSAT only uses solar radiation, and minimum and maximum temperature to calculate reference evapotranspiration (ETo) using the Priestley-Taylor equation. In order to keep the datasets as similar as possible between AquaCrop and DSSAT no additional relative humidity and wind speed data from other data sources were added. ETo Calculator (Raes, 2009) was used to calculate daily ETo values based on the available data.

Daily rainfall was measured on each site in Togo using manual rain gauges. Daily minimum and maximum temperatures, air humidity, and wind speed data were provided by the nearest weather station at Lomé (6.1256°N; 1.2254°E; 19.6 msl) for Sevekpota and Tabligbo weather

Table 1
Overview and synthesis of the available cassava field data, (Col: Colombia; Tgo: Togo; Nga: Nigeria).

Site	Variety	Planting date [dd-mm-yyyy]	Irrigated [dimensionless]	Length season [days]	Sowing density [plants/ha]	# Canopy cover obs. [dimensionless]	# Biomass obs. [dimensionless]	Water stress [dimensionless]	Cal/Val** [dimensionless]
Palmira (Col)	MCol-1684	15–12–1978	Yes	362	10,000	11	6	No	Cal
Palmira (Col)	MCol-22	15–12–1978	Yes	362	10,000	11	6	No	Cal
Palmira (Col)	MVen-77	15–12–1978	Yes	362	10,000	11	6	No	Val
Palmira (Col)	MPtr-26	15–12–1978	Yes	362	10,000	11	6	No	Cal
Palmira (Col)	MCol-1684	13–07–1979	No	178	10,000	5	5	No	Cal
Palmira (Col)	MCol-22	13–07–1979	No	178	10,000	5	5	No	Val
Palmira (Col)	MVen-77	13–07–1979	No	178	10,000	5	5	No	Cal
Palmira (Col)	MPtr-26	13–07–1979	No	178	10,000	5	5	No	Cal
Palmira (Col)	MCol-1684	29–01–1980	Yes	303	10,000	10	4	No	Val
Palmira (Col)	MCol-638	29–01–1980	Yes	303	10,000	10	4	No	Cal
Palmira (Col)	MMex-59	29–01–1980	Yes	303	10,000	10	4	No	Cal
Palmira (Col)	MPtr-26	29–01–1980	Yes	303	10,000	10	4	No	Val
Sevekpota (Tgo)	TME-419	22–05–2012	No	317	15 625	6	3	Yes	Val
Sevekpota (Tgo)	TME-419	23–04–2013	No	322	15 625	8	3	Yes	Cal
Djakakope (Tgo)	TME-419	22–05–2012	No	318	15 625	6	1	Yes	Cal
Djakakope (Tgo)	TME-419	03–05–2013	No	322	15 625	8	3	Yes	Val
Ogoja (Nga)	TME-419	16–06–2016	No	265*	12 500	–	2	Yes	Cal
Otukpu (Nga)	TME-419	17–08–2016	No	265*	12 500	4	2	Yes	Cal
Ekpoma (Nga)	TME-419	12–05–2017	No	265*	12 500	4	2	No	Cal
Ikom (Nga)	TME-419	03–06–2017	No	265*	12 500	–	1	No	Val
Otukpo (Nga)	TME-419	15–06–2017	No	265*	12 500	3	2	Yes	Val

* Simulations stopped at 265 DAP before dormancy at the end of the 1st growing cycle.
** Cal/Val: calibration or validation dataset.

station (6.583°N; 1.500°E; 40 msl) for Djakakope. Daily solar radiation was not measured in the area and therefore satellite data provided by the NASA (Langley Research Center (LaRC)) POWER ('Prediction Of Worldwide Energy Resources') project were used (funded through the NASA Earth Science/Applied Science Program; NASA LaRC, 2022). ETo was calculated following the modified Penman-Monteith equation (Allen et al., 1998) using ETo Calculator (Raes, 2009).

For Nigeria weather data were obtained from nearby weather stations for Ekpoma (6.7491°N; 6.0732°E; 214 msl), Ogoja (6.6548°N; 8.7977°E; 47 msl), Ikom (5.9617°N; 8.7206°E; 105 msl) and Otukpo (7.1982°N; 8.1393°E; 139 msl). Data included maximum and minimum temperature, and precipitation. Wind speed, vapour pressure and solar radiation also had to be retrieved from the NASA (LaRC) POWER website to calculate ETo using the modified Penman-Monteith equation.

An overview of the total seasonal or growing period rainfall and ETo observations for the different study sites is given in Table 2.

2.2.2. Soil data

The Colombian experiments were carried out on CIAT's experimental fields in Palmira, near Cali. All trials were run on the same fertile Clay Loam soil, classified as a Mollisol (FAO, 2014). Soil hydraulic properties for different soil layers (0–200 cm) were retrieved from

Table 2
Growing season total rainfall and ETo observations.

	Total seasonal rainfall [mm]	Total seasonal ETo [mm]		Total seasonal rainfall [mm]	Total seasonal ETo [mm]
Palmira 1978 (Col)	867	1 572	Djakakope 2013 (Tgo)	659	716
Palmira 1979 (Col)	458	754	Ekpoma 2017 (Nga	1 667	736
Palmira 1980 (Col)	595	1 431	Ikom 2017 (Nga)	1 720	675
Sevekpota 2012 (Tgo)	574	478	Ogoja 2016 (Nga)	1 234	605
Sevekpota 2013 (Tgo)	731	640	Otukpo 2016 (Nga)	655	360
Djakakope 2012 (Tgo)	736	633	Otukpo 2017 (Nga)	963	489

DSSAT. Since the soil layer characteristics differed only slightly, a uniform soil layer was assumed for AquaCrop (Table 3).

In Togo, tests were conducted on an Acrisol (FAO, 2014) with a hard pan at about 50–80 cm in Sevekpota, and a Ferralsol (FAO, 2014) with a depth over 200 cm in Djakakope. The provided dataset included organic characteristics and soil texture measurements. Saxton pedo-transfer functions (Saxton and Rawls, 2006) were used to convert them into soil hydraulic properties (Table 3).

Soil characteristics for the Nigerian cassava studies are also presented in Table 3. The soils in Ekpoma, Ogoja and Ikom are classified as Nitisol (FAO, 2014); and as Acrisol (FAO, 2014) in Otukpo. Soil particle distribution measurements were available for each field and they were used to calculate the required soil hydraulic properties with Saxton pedo-transfer functions (Saxton and Rawls, 2006).

2.2.3. Crop data

Different varieties were included in the Colombian field trials: MCol-1684, MCol-638, MCol-22, MMex-26 MPtr-26 and MVen-77. With 'M' referring to *Manihot esculenta*; and 'Col' for Colombia, 'Mex' for Mexico, 'Ptr' for Puerto Rico and 'Ven' for Venezuela. All these varieties have quite different characteristics from high yielding (e.g. MCol-1684, MMex-59) to stress resistant (e.g. MCol-638, MMex-59), and late branching (e.g. MPtr-26, MVen-77) (CIAT, 1980; Veltkamp, 1985; Ospina et al., 2016). TME-419 is a more recent, locally popular, improved cassava variety in Togo (also called "Gbazekoute") and in Nigeria (Ezui et al., 2018; Adiele et al., 2021).

Data collection on biomass yield was done for all plots at several times throughout the growing season. Each time storage roots, stems, fresh and fallen leaves were collected and oven dried at 78–80 °C until constant weight (Veltkamp, 1985; Ezui, 2017). Table 4 shows an overview of the mean dry matter biomass weights; comprising the sum of storage root, stem, fresh and fallen leaves dry weight at different days after planting (DAP). The final storage root dry matter yield is also given. Since AquaCrop converts biomass into yield only at the end of the growing season, intermediate harvest yield measurements are not needed. The lower yields are mainly due to reported water shortages: e.g. 55% losses due to drought in Sevekpota (Togo) in 2012 (Ezui et al., 2018), and severe and moderate water stresses due to prolonged dry spells in Otukpo (Nigeria) in 2016 and 2017 (Adiele et al., 2021) (see also seasonal rainfall totals in Table 2).

No direct fractional green canopy cover (CC) observations were available. However, it can be assumed that light interception percentage and CC are nearly identical, as shown for potatoes by Van Der Zaag (1984). In Colombia, canopy light interception percentages were derived from above and beneath canopy global solar radiation measurements using a Licor LI-170 quantum meter (Lambda Instruments Corporation) (Veltkamp, 1985). On the plots in Togo and Nigeria, LAI was measured using Decagon's AccuPAR LP-80 PAR/LAI Ceptometer (Ezui, 2017). Light interception can also be retrieved from LAI observations through the Lambert-Beer equation described in Monsi and Saeki (2005) (Eq. (3)). The resulting mean fractional green canopy cover values for the ensemble plots at different DAPs are presented in Table 5.

$$\%\text{light intercepted} = \frac{I}{I_o} = 1 - e^{-k \cdot LAI} \quad (3)$$

where:

I: light received at about 20 cm above the soil surface [MJ m^{-2}].

I_o: incoming light above the crop canopy [MJ m^{-2}].

LAI: leaf area index [dimensionless].

k: extinction coefficient (0.67 for TME-419 (Ezui, 2017)) [dimensionless].

The trials in Colombia for 1979, Togo and Nigeria were all rainfed. For the irrigated fields (in Colombia for 1978 and 1980), net irrigation amount and times of application were specified in DSSAT. Fertilizer applications were considered optimal for all fields. Sowing densities, planting and harvest dates for the ensemble of plots were also provided (Table 1). As for the lengths of the growing season, on most fields, cassava was grown for only one cycle of 10–12 months. Only the Nigerian trials covered several cycles: first cycle, drought induced dormancy, regrowth and second growing cycle. In the present study, only the first cycle until the end of the dormancy period was simulated.

3. Results and discussion

3.1. Calibration and validation results

A single cassava crop parameter file was created for the ensemble datasets (Table 6). Three levels of parameters are given. Table 6. A presents the conservative parameters; they are crop specific and largely independent of management or agroclimatic zone. Cultivar dependent crop parameters are proposed in Table 6. C; they were successfully calibrated and validated for the present case studies, but can vary with

Table 3
Soil hydraulic properties for the different pilots and for different soil layers (if applicable).

	Thickness [m]	PWP [vol%]	FC [vol%]	SAT [vol%]	Ksat [mm/day]	Penetrability [%]
Palmira (Col)						
Clay loam	2.0	26.5	40.3	52.5	105.6	100
Sevekpota 2012 (Tgo)						
Sandy clay loam	0.2	18.8	29.6	42.5	126.2	100
Clay	0.2	27.0	39.0	45.4	15.6	100
Clay	0.4	32.0	44.3	48.9	6.0	75
Hard pan at ± 50–80 cm	1.2	0.1	0.3	0.5	0.0	35
Sevekpota 2013 (Tgo)						
Sandy loam	0.2	11.0	19.2	40.8	585.4	100
Sandy clay loam	0.2	20.1	30.1	41.1	76.8	100
Sandy clay	0.4	24.8	35.8	43.0	22.1	75
Hard pan at ± 50–80 cm	1.2	0.1	0.3	0.5	0.0	35
Djakakope 2012–2013 (Tgo)						
Silt loam	2.0	8.0	23.0	46.0	55.0	100
Ekpoma 2017 (Nga)						
Sandy loam	0.3	10.0	22.0	41.0	1 200	100
Loamy sand	1.7	14.8	31.0	46.0	1 300	100
Ogoja 2016 and Ikom 2017 (Nga)						
Sandy Loam	2.0	15.0	31.0	46.0	712.0	100
Otukpo 2016–2017 (Nga)						
Sandy loam	1.6	11.0	36.2	48.7	797.5	100
Clay	0.4	39.0	54.0	55.0	35.0	20

Table 4
Observed dry weight biomass and their days after planting (DAP),and final root tuber yield for the different pilots.

Site	Variety	Year		DAP & Biomass[days]; [tonne/ha]						Yield [tonne/ha]
			DAP	63	123	185	241	304	362	
Palmira (Col)	MCol-1684	1978	Weight (DM)	1.2	7.6	17.8	19.8	24.4	27.1	14.4
	MCol-22		Weight (DM)	1.2	7.1	14.9	19.0	23.4	27.1	13.0
	MVen-77		Weight (DM)	1.2	7.6	16.4	19.6	22.0	26.3	10.4
	MPtr-26		Weight (DM)	1.1	7.5	15.7	18.6	21.3	26.1	13.6
			DAP	48	73	88	117	175		
Palmira (Col)	MCol-1684	1979	Weight (DM)	0.7	1.6	2.7	4.6	12.1		4.6
	MCol-22		Weight (DM)	0.5	1.2	2.3	5.1	8.8		5.1
	MVen-77		Weight (DM)	0.8	1.7	2.9	5.8	12.8		5.7
	MPtr-26		Weight (DM)	0.8	1.9	3.4	5.6	12.5		5.5
			DAP			138	185	246	303	
Palmira (Col)	MCol-1684	1980	Weight (DM)			7.8	13.6	20.4	19.8	11.8
	MCol-638		Weight (DM)			6.0	10.8	14.3	13.7	4.4
	MMex-59		Weight (DM)			6.4	11.7	21.1	22.9	7.4
	MPtr-26		Weight (DM)			8.8	13.3	20.8	22.0	11.7
			DAP			127		245	317	
Sevekpota (Tgo)	TME-419	2012	Weight (DM)			2.4		10.8	11.3	4.9
			DAP			139		238	322	
Sevekpota (Tgo)	TME-419	2013	Weight (DM)			9.8		18.4	22.2	9.9
			DAP						328	
Djakakope (Tgo)	TME-419	2012	Weight (DM)						17.8	8.0
			DAP			136		231		
Djakakope (Tgo)	TME-419	2013	Weight (DM)			10.0		16.9		10.5
			DAP			137		252		
Ogoja (Nga)	TME-419	2016	Weight (DM)			13.1		15.3		8.9
			DAP			151		227		
Otukpu (Nga)	TME-419	2016	Weight (DM)			4.7		4.5		3.8
			DAP			144		247		
Ekpoma (Nga)	TME-419	2017	Weight (DM)			18.8		24.0		11.4
			DAP					239		
Ikom (Nga)	TME-419	2017	Weight (DM)					18.6		9.9
			DAP			139		250		
Otukpo (Nga)	TME-419	2017	Weight (DM)			7.0		11.6		6.7

Table 5
Canopy cover (CC) observations and their days after planting (DAP) for the different pilots.

Site	Variety	Year		DAP [days] & Canopy cover [%]										
			DAP	62	92	123	151	185	213	241	279	304	335	360
Palmira (Col)	MCol-1684	1978	CC	50.2	92.8	93.0	95.0	92.4	62.1	53.3	60.2	81.0	85.0	79.9
	MCol-22		CC	48.3	87.9	86.4	91.4	93.5	49.0	48.5	58.3	73.0	72.8	70.9
	MVen-77		CC	46.6	89.7	89.6	92.4	91.4	54.0	49.6	56.6	69.3	76.4	62.3
	MPtr-26		CC	33.0	76.9	91.3	93.6	95.4	80.1	78.8	90.9	92.1	92.4	85.1
			DAP	48	73	88	117	175						
Palmira (Col)	MCol-1684	1979	CC	27.6	60.1	79.4	79.2	82.5						
	MCol-22		CC	18.8	48.1	69.3	76.8	76.1						
	MVen-77		CC	22.9	70.2	81.8	86.6	72.3						
	MPtr-26		CC	19.0	51.4	71.3	81.2	83.8						
			DAP	73	96	125	152	171	194	229	246	275	303	
Palmira (Col)	MCol-1684	1980	CC	46.4	67.1	91.0	96.1	77.0	81.0	65.0	62.6	71.1	58.9	
	MCol-638		CC	2.0	60.0	94.0	97.9	94.8	94.7	90.9	90.0	86.7	89.9	
	MMex-59		CC	9.0	45.0	72.1	92.7	86.7	91.9	93.9	93.7	95.5	88.6	
	MPtr-26		CC	53.9	71.9	86.7	92.7	61.7	76.7	59.8	68.7	77.5	55.5	
			DAP		91	122	152	183		213	243			
Sevekpota (Tgo)	TME-419	2012	CC		48.0	48.8	78.7	86.7		73.3	27.5			
			DAP		100		149	170	201	225	265	301	320	
Sevekpota (Tgo)	TME-419	2013	CC		97.3		83.3	77.2	75.1	46.3	15.2	12.9	57.4	
			DAP		91	122	152	183	213	243				
Djakakope (Tgo)	TME-419	2012	CC		67.0	73.3	80.7	84.9	70.1	45.2				
			DAP		103	131		173	204	222	259	298	320	
Djakakope (Tgo)	TME-419	2013	CC		76.1	81.6		64.2	65.8	71.6	45.2	42.5	52.4	
			DAP											
Ogoja (Nga)	TME-419	2016	CC											
			DAP	37	78	120				242				
Otukpu (Nga)	TME-419	2016	CC	16.2	30.2	44.6				34.0				
			DAP	30	76	122				243				
Ekpoma (Nga)	TME-419	2017	CC	22.0	84.5	99.0				67.3				
			DAP											
Ikom (Nga)	TME-419	2017	CC											
			DAP		76	122				243				
Otukpo (Nga)	TME-419	2017	CC		70.3	82.0				31.9				

Table 6
Detailed AquaCrop cassava crop parameters.

Crop parameter	Value	Method of Determination
A. Conservative and/or crop specific parameters		
Base temperature (°C)	10.0	L
Upper temperature (°C)	30.0	L
Soil water depletion factor for canopy expansion (p-exp) - Upper threshold	0.25	C
Soil water depletion factor for canopy expansion (p-exp) - Lower threshold	0.60	C
Shape factor for water stress coefficient for canopy expansion	3.0	D
Soil water depletion fraction for stomatal control (p-sto) - Upper threshold	0.50	C
Shape factor for water stress coefficient for stomatal control	3.0	D
Soil water depletion factor for canopy senescence (p-sen) - Upper threshold	0.50	C
Shape factor for water stress coefficient for canopy senescence	3.0	D
vol% for Anaerobiotic point (* (SAT - [vol %]) at which deficient aeration occurs *)	5	D
Canopy growth coefficient (CGC): Increase in canopy cover (fraction soil cover per day)	0.10425	C
Canopy decline coefficient (CDC): Decrease in canopy cover (in fraction per day)	0.04100	C
Crop coefficient when canopy is complete but prior to senescence ($K_{c,Tr,x}$)	0.85	C
Decline of crop coefficient (%/day) as a result of ageing, nitrogen deficiency, etc.	0.050	C
Water Productivity normalized for ETo and CO_2 (WP*) (gram/m^2)	17.0	C
Possible increase (%) of HI due to water stress before start of yield formation	4	C
Coefficient of positive impact on HI of restricted vegetative growth during yield formation	4.0	C
Coefficient of negative impact on HI of stomatal closure during yield formation	10.0	C
Allowable maximum increase (%) of specified HI	15	C
B. Non-tested crop specific parameters		
Minimum growing degrees required for full crop transpiration (°C - day)	11.1	C
Minimum and maximum air temperature below which pollination starts to fail	–	NA
Response to soil fertility	–	NA
Soil salinity stress	–	NA
C. Non-conservatives and/or cultivar specific parameters		
Calendar Days from transplanting to recovered transplant	10	E
Calendar Days from transplanting to maximum rooting depth	70	E
Calendar Days from transplanting to start senescence	300	E
Calendar Days from transplanting to maturity	360	E
Calendar Days from transplanting to start of yield formation	80	E
Minimum effective rooting depth (m)	0.30	D
Maximum effective rooting depth (m)	1.00	L
Shape factor describing root zone expansion	1.50	D
Maximum root water extraction (m^3 water/m^3 soil.day) in top quarter of root zone	0.048	D
Maximum root water extraction (m^3 water/m^3 soil.day) in bottom quarter of root zone	0.013	D
Effect of canopy cover in reducing soil evaporation in late season stage	60	E
Soil surface covered by an individual seedling at 90% emergence (cm^2)	10.00	M
Number of plants per hectare	10,000–15,625	M
Maximum canopy cover (CCx) in fraction soil cover	0.77–0.99	M
Building up of Harvest Index starting at root/tuber enlargement (days)	250	C
Reference Harvest Index (HIo) (%)	60	C

C: calibration; D: AquaCrop default; E: estimation; L: literature; M: measured; NA: not applicable.

cultivar and location (Steduto et al., 2012). Parameters to simulate the effects of temperature, soil fertility and soil salinity stresses could not be determined using the available datasets (Table 6B) The parameters of Table 6 realistically represent cassava physiology and production system, and are in line with the recent review by Cock and Connor (2021). Firstly, cassava has a relatively high photosynthetic rate among C3 crops, hence the relatively high WP* that was selected. Regarding the transpiration coefficient, $K_{c,Tr}$, Cock and Connor (2021) provided evidence of substantial midday stomatal closure in response to vapour pressure deficit (VPD) in cassava (under non-limiting soil water), and also reported a decoupling coefficient for cassava of 0.2, indicating strong control of transpiration via reduced canopy conductance. Therefore, a $K_{c,Tr}$ below 1.0 was chosen to better simulate the regulation of transpiration by cassava canopies. Fig. 1 confirms these parameter values. For the ensemble of water unlimited fields, biomass measurements normalized for CO_2 were plotted against the cumulative normalized transpiration, with a regression line slope (equivalent to the WP*) of 17 (g/m^2) and an R^2 of 0.97. Finally, by adding the water limited datasets, the finetuning of stress coefficients led to the selection of a high threshold for the Ks_{sto} value, given the sensitivity of cassava stomata to water status (Cock and Connor, 2021 and references therein).

Some simulation results, taken from the calibration and validation datasets, are presented in Fig. 2. The left-side figures show the simulated (black line) vs observed fractional green canopy cover (grey dots). The water balance for each field is presented in the middle of Fig. 2. The depletion rate in the soil profile (black line) is depicted against the depletion rates at field capacity (i.e. 0) and permanent wilting point (grey lines); the potential and actual depletion rates increase with root zone development along the growing season. Rainfall (blue columns) and/or irrigation (light green columns) contributions are added as well. The different water stress threshold levels are also shown. If the depletion rate drops below these thresholds, water stress kicks in affecting canopy development (green threshold line), stomatal closure (red line) and early senescence (orange line). On the right are presented dry matter biomass simulations (black line) vs observations (grey dots) along the growing season, expressed in days after planting (DAP). Each

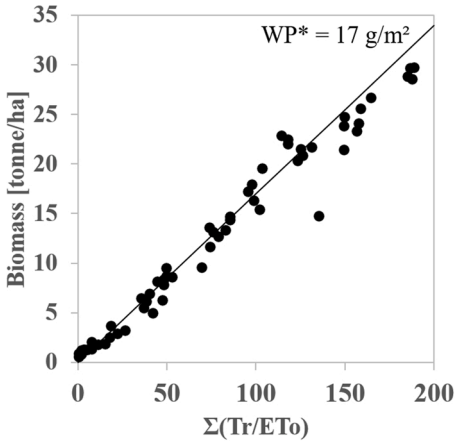

Fig. 1. Relationship between biomass (normalized for CO2) and cumulative transpiration (normalized for ETo) for the ensemble of water unlimited cassava fields (black dots). Black line represents the WP* of 17 g/m^2.

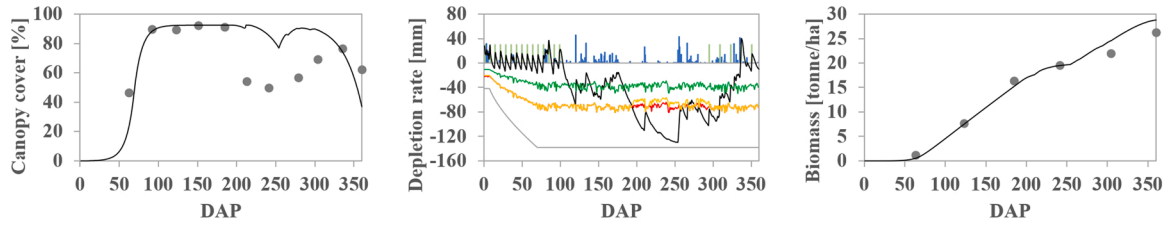

a) Mven-77 variety for Palmira (Col) 1978 (validation dataset)

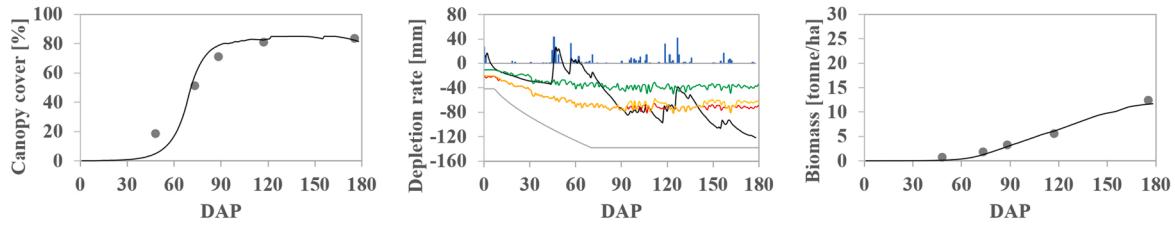

b) MPtr-26 variety for Palmira (Col) 1979 (calibration dataset)

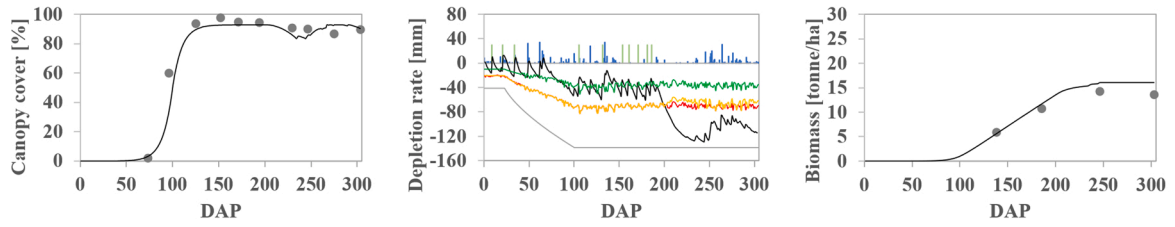

c) MCol-638 variety for Palmira (Col) 1980 (calibration dataset)

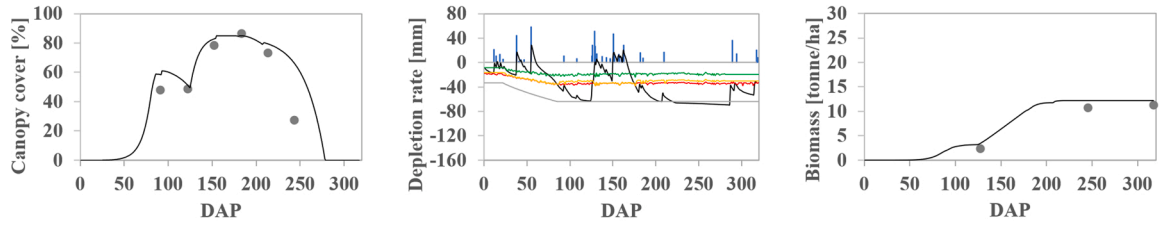

d) TME-419 variety for Sevekpota (Tgo) 2012 (validation dataset)

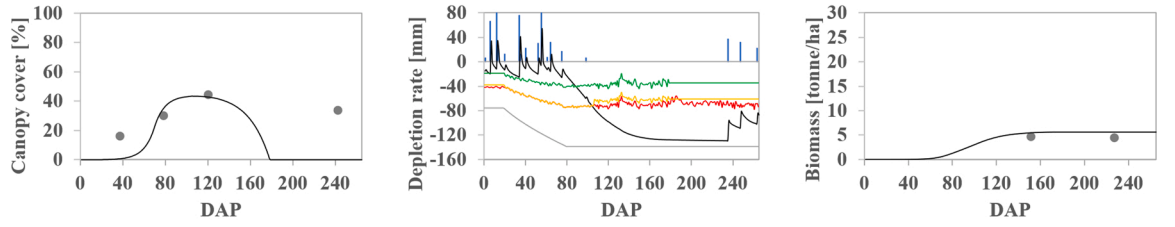

e) TME-419 variety for Otukpo (Nga) 2016 (calibration dataset)

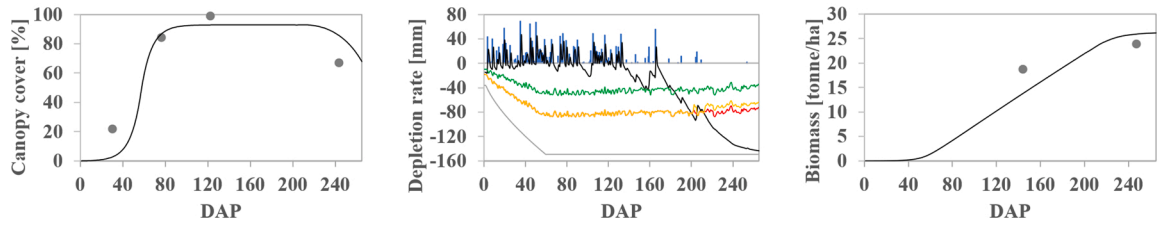

f) TME-419 variety for Ekpoma (Nga) 2017 (calibration dataset)

Fig. 2. a–e – Some AquaCrop simulations results. Left: simulated (black line) and observed (grey dots) canopy cover development. Middle: Simulated depletion rate (black line), depletion rated at saturation and permanent wilting point (grey lines), irrigation and rainfall events (blue and light green columns), and water stress thresholds (impacting: green: development, red: stomatal closure, orange: early senescence) Right: Observed (black line) vs simulated dry biomass production (grey dots) (DAP: days after planting). (For interpretation of the references to colour in this figure legend, the reader is referred to the web version of this article.)

line gives a comprehensive overview of the water-soil-plant interactions for each field.

At the moment (for instance in the case of field MVen-77 of 1978 (Colombia)), AquaCrop was not fully able to simulate the canopy cover drop produced by leaf shedding because of prolonged drought, clearly visible in the water balance. But this drop in canopy activity is nevertheless very nicely translated in a pause of biomass production, which is the final objective i.e. to simulate biomass and yield responses to water. In Sevekpota (Togo), during the 2012 growing season, the onset of a second growing cycle was from 220 to 240 days after planting. Soil moisture increases in the water balance and canopy cover also re-develops; AquaCrop is however not yet capable of simulating multiple cycles. Nevertheless, given the differences in studied cases (different varieties, field managements and agro-ecological regions), AquaCrop handled the crop simulations very well; see Figs. 2–4 and Table 7.

Fig. 3 and Table 7 show the calibration and validation results for simulated and observed final dry matter biomass. Calibration and validation yielded an R^2 of 0.96 and 0.87 respectively. The root-mean-square errors (RMSE) and its variations were also satisfyingly low. Calibration and validation of the yield estimates were slightly more complicated (Fig. 4 and Table 7). Given the different varieties in the Colombian dataset, it was not possible to find a single HI value. The growth characteristics of these varieties differ, with limited data per variety. Table 8 proposes a mean HIo of 45% for the varieties grown in Colombia; indicative values for the different varieties are also given. For the TME-419 variety (HIo of 60%) of Togo and Nigeria, in both cases, results were good with a calibration R^2 of 0.94 and a validation R^2 of 0.95.

3.2. Discussion

AquaCrop has proven to be a robust and solid crop-water productivity model requiring limited, easily interpretable and obtainable data. A unique cassava crop-file was parametrized, calibrated and validated for different varieties and agro-ecological regions using ‘first degree’ (biomass and yield) and ‘second degree’ (climate, soil and canopy cover) data. The model also performed well in simulating biomass and yield, obtained from other similar studies. However, standard deviations in the observed data were often missing and hence overall omitted. Available climate, soil and canopy cover data were not fully adapted for AquaCrop. Additional climate variables had to be downloaded from the NASA (LaRC) POWER site in order to calculate daily ETo values which are critical in AquaCrop. NASA POWER satellite-based data can replace missing weather data, but caution must be taken as these data can sometimes be unreliable (Marzouk, 2021). As for the soil data, none of them contained saturated hydraulic conductivity (Ksat) measurements,

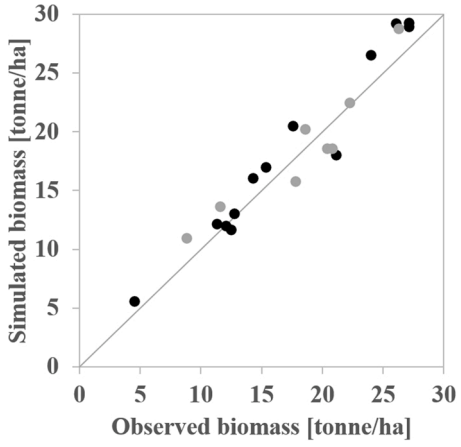

Fig. 3. Observed vs simulated dry biomass (black dots: calibration, grey dots: validation.

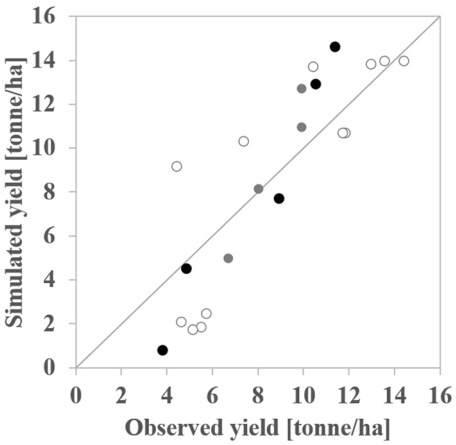

Fig. 4. Observed vs simulated dry tuber yield(black dots: TME-419 calibration, grey dots: TME-419 validation, white dots: ensemble varieties grown in Colombia).

Table 7
Calibration and validation metrics for cassava biomass and final dry tuber yield (HIo = 60% for TME-419; HIo = 45% for varieties grown in Colombia).

		R^2 [dimensionless]	RMSE [tonne DM/ha]	rRMSE [%]	nRMSE [%]
Biomass	calibration	0.96	1.99	2.69	11.46
	validation	0.87	1.94	2.30	10.58
Yield MCol-22, MCol-638, MCol-1684	calibration	0.71	2.80	3.82	32.68
MMex-59, MPtr-26, MVen-77	validation	0.78	2.49	2.80	25.47
Yield TME-419	calibration	0.94	2.37	2.87	29.99
	validation	0.95	1.74	2.77	20.13

Table 8
Varieties and their reference harvest indices (HIo)(left part of table: HIo for TME-419 and the ensemble of varieties grown in Colombia;right part of the table: individual HIo values for the varieties grown in Colombia).

Cultivar	Observations [dimensionless]	HIo [%]	Cultivar	Observations [dimensionless]	HIo [%]
TME-419	10	60	MCol-22	2	45
Ensemble of varieties grown in Colombia	12	45	MCol-638	1	25
			MCol-1684	3	48
			MMex-59	1	30
			MPtr-26	3	45
			MVen-77	2	40

only for some fields soil hydraulic properties were provided and the number of soil layers and their depths varied between the different datasets and even between fields within the same dataset. However, for all fields granulometric sand and clay mass distributions were given, so all the needed soil hydraulic properties were derived in AquaCrop using Saxton transfer functions (Saxton and Rawls, 2006) and where needed soil profiles were simplified to a simple soil profile of 2 m depth. Fractional green canopy cover measurements were not available and had to be derived from measured light interception and LAI. For future fine-tuning, aerial image traits analysis offers promising results to directly assess fractional green canopy cover (Selvaraj et al., 2020).

Despite all these simplifications, the cassava simulations with AquaCrop model performed well. We expect this present paper will simulate further calibration efforts with additional experimental datasets in different environments to confirm or modify our proposed crop parameter file.

The crop stress factors could not be calibrated based on soil moisture measurements, since they were not available. However, the most important components of the soil-water balance were available in a detailed and accurate way to properly simulate it. Namely, the: i) total available water (TAW) in the root zone, ii) precipitation and/or irrigation, and iii) crop transpiration. AquaCrop expresses the impact of water limitation as a fraction of TAW, the difference between water content at field capacity and permanent wilting point, in the root zone (Steduto et al., 2012). These soil hydraulic properties, including saturated hydraulic conductivity, were derived for each field by means of pedotransfer functions. Precipitation was measured daily in rain gauges near the different fields, and irrigation doses and dates were specified, if applied. Crop transpiration was correctly calibrated, as shown priorly in Fig. 1. As a consequence, the crop stress factors were indirectly estimated from soil water balance simulations, and visual interpretation of canopy cover and biomass evolutions. Nevertheless, soil moisture observations could have improved the calibration and validation of these stress factors.

Harvest index (HI) was only calibrated and validated for the TME-419 variety. For the cassava varieties grown in Colombia, storage root yields varied widely among different varieties, so no satisfactory single HI could be proposed for this ensemble of varieties. In AquaCrop a reference HI (HIo) is variety dependent but there were not enough observations for each variety to assess the specific HIo values of the different varieties. However, since AquaCrop calculates storage root yield from biomass at the end of the growing season (and not per intermediate harvest along the growing season), these parameters can be easily obtained by minor additional field measurements by those wanting to further adapt the present cassava crop-file for their specific varieties.

The actual version of AquaCrop does not yet simulate cassava's typical multiple growing cycles with intermediate dormancy. Except for the Nigerian data, none of the datasets covered multiple growing cycles. The simulation of these fields was stopped during the dormancy phase. For the other and major part of the fields, simulations ran until harvest (covering one growing cycle). An option could have been to parametrize an additional crop-file to simulate this second growing cycle, as was done for sugarcane by Wellens et al. (2020). Presently, there is not enough data available to properly calibrate and validate such a second-growth cassava crop-file.

Though every model has its advantages and disadvantages, strengths and weaknesses, AquaCrop stacked up very successfully with other existing cassava models. The MANIHOT-Cassava model, incorporated in DSSAT and originally developed on the Veltkamp (1985) dataset, obtained an average biomass RMSE of 3.3 tonnes DM/ha for some of the varieties used (MCol-1684, MCol-22, MPtr-26 and MVen-77) (Moreno Cardena, 2018) and also for one growing cycle. Using the parameter rich LINTUL-Cassava model, Ezui et al. (2018) obtained an overall R^2 close to 1, and an nRMSE of 6.6% for total biomass production and 5.8% for final storage roots yield. Their work concentrated on 4 trials in Southern-Togo, with the same TME-419 variety but for two growing cycles. Adiele et al. (2021) recalibrated LINTUL-Cassava model and validated it using data obtained from 5 different fields with the same TME-419. An R^2 of 0.92 and a RMSE of 4.93 tonnes DM/ha was attained for the storage root yields at 4 months after planting (MAP) (vegetative period), 8 MAP (mid-season) and at final harvest.

4. Conclusion

Increasing yield and water use efficiency is becoming increasingly important when cultivating crops in climate change-vulnerable regions. In this context AquaCrop was calibrated and validated for cassava. A single crop-file was able to cover different varieties and agro-ecological regions. For some cases, minor and easily obtainable modifications might be needed to better adapt the crop-file to local conditions. Albeit based on different qualitative datasets, a rigorous calibration and validation procedure was successfully achieved. Also, it was shown that missing data, replaced from third parties or data conversion/transfer procedure, had almost no impact on the final simulations. The resulting crop-file can be applied with confidence in further studies concentrating on improved water and/or field management to produce more "crop with every drop", and so be an important new tool in mitigating the impact of a changing climate on cassava production.

Declaration of Competing Interest

The authors declare that they have no known competing financial interests or personal relationships that could have appeared to influence the work reported in this paper.

Acknowledgments

This study was made possible thanks to the International Atomic Energy Agency (IAEA), through the Consortium for Improving Agriculture-based Livelihoods in Central Africa (CIALCA; www.cialca.org) and the regional IAEA Technical Cooperation Project RAF5081 on Enhancing Productivity and Climate Resilience in Cassava-Based Systems through Improved Nutrient, Water and Soil Management. The Joint FAO/IAEA Centre of Nuclear Techniques in Food and Agriculture coordinated the research and facilitated the exchanges between different researchers and their institutes. Special thanks go to the International Fertilizer Development Centre (IFDC), and the Consultative group for International Agricultural research (CGIAR), through its organizations IITA and CIAT for their effortless sharing of data and expert knowledge. All data are made available for download at GitHub (https://github.com/Joost-Wellens/AquaCrop_cassava_data). The cassava crop file will also be made available in the upcoming new version 7.0 of AquaCrop (www.fao.org/aquacrop).

References

Abdoul-Hamid, M.S., Tychon, B., Piccard, I., Gobin, A., Van Hoolst, R., Djaby, B., Wellens, J., 2019. Batch-processing AquaCrop plug-in for rainfed maize using satellite derived Fractional Vegetation Cover data. Agr. Water Manag. 217, 346–355. https://doi.org/10.1016/j.agwat.2019.03.016.

Adiele, J.G., Schut, A.G.T., van den Beuken, R.P.M., Ezui, K.S., Pypers, P., Ano, A.O., Egesi, C.N., Giller, K.E., 2021. A recalibrated and tested LINTUL-Cassava simulation model provides insight into the high yield potential of cassava under rainfed conditions. Eur. J. Agron. 124, 126242 https://doi.org/10.1016/j.eja.2021.126242.

Allen, R., Pereira, L.S., Raes, D., Smith, M., 1998. Crop evapotranspiration-guidelines for computing crop water requirements. FAO Irrigation and Drainage Paper 56.FAO, Rome, Italy. p. 300. ⟨https://www.fao.org/3/x0490e/x0490e00.htm⟩ (Accessed 10 January 2022).

CIAT, 1980. Annual Report Cassava Program for 1979. Centro Internacional de Agricultura Tropical, Cali, Colombia.

Cock, J.H., Connor, D.J., 2021. Cassava. In: Sadras, V., Calderini, D. (Eds.), Crop Physiology Case Histories for Major Crops. Academic Press, pp. 588–633. https://doi.org/10.1016/C2018-0-05018-5.

Ezui, K.S., 2017. Understanding the productivity of cassava in West-Africa. Ph.D. Dissertation. Wageningen University, Netherlands, p. 183.

Ezui, K.S., Leffelaar, P.A., Franke, A.C., Mando, A., Giller, K.E., 2018. Simulating drought impact and mitigation in cassava using the LINTUL model. Field Crops Res. 219, 256–272. https://doi.org/10.1016/j.fcr.2018.01.033.

FAO, 2014. World Reference Base for Soil Resources 2014: International soil classification system for naming soils and creating legends for soil maps. FAO, Rome,, Italy, p. 106. ⟨https://www.fao.org/soils-portal/data-hub/soil-classification/world-reference-base/en/⟩ (Accessed 10 January 2022).

Geerts, S., 2008. Deficit Irrigation Strategies Via Crop Water Productivity Modelling: Field Research of Quinoa in the. KU Leuven University, Belgium.

Geerts, S., Raes, D., Garcia, M., 2010. Using AquaCrop to derive deficit irrigation schedules. Agr. Water Manag. 98 (1), 213–216. https://doi.org/10.1016/j.agwat.2010.07.003.

Hoogenboom, G., Porter, C.H., Shelia, V., Boote, K.J., Singh, U., White, J.W., Hunt, L.A., Ogoshi, R., Lizaso, J.I., Koo, J., Asseng, S., Singels, A., Moreno, L.P., Jones, J.W., 2018. Decision support system for agrotechnology transfer (DSSAT) version 4.7.5.

DSSAT Foundation, Gainesville, Florida, USA.⟨https://DSSAT.net⟩ (Accessed 10 January 2022).

Kiptum, K., Kipkorir, E.C., Munyao, T.M., Ndambuki, J.M., 2013. Application of AquaCrop model in deficit irrigation management of cabbages in Keiyo Highlands. Int. J. Water Res. Environ. Eng. 5 (7), 360–369. ⟨https://academicjournals.org/journal/IJWREE/edition/July_2013⟩ (Accessed 10 January 2022).

Kumsueb, B., Jintrawet, A., 2020. Recent evaluations and applications of a cassava model in Thailand: a review. Curr. Appl. Sci. Technol. 20 (1), 156–162. ⟨https://li01.tci-thaijo.org/index.php/cast/article/view/226425⟩ (Accessed 10 January 2022).

Lebot, V., 2008. Tropical root and tuber crops: Cassava, sweet potato, yams and aroids. In: Rees, J., Atherton, A. (Eds.), "Crop Production Science in Horticultures Series", 17. CABI.

López-Lavalle, L.A.B., Andrade, R.S., Rivera, T., Campaz, B., Newby, J., Lourido, D., Gutiérrez, D., Carciá, C., Mwanzia, L., Pino, L., Muriel, O., Tohme, J., 2021. Cassava Lighthouse: Monitoring Open Access data for the Cassava Sector. Version 1. 0 2021.⟨https://cassavalighthouse.org/about⟩ (Last Accessed 03 August 2021).

Marzouk, O.A., 2021. Assessment of global warming in Al Buraimi, Sultanate of Oman, based on statistical analysis of NASA POWER data over 39 years, and testing the reliability of NASA POWER against meteorological measurements. Heliyon 7 (3), e06625. https://doi.org/10.1016/j.heliyon.2021.e06625.

Moreno Cadena, L.P., 2018. Modelo de la simulación de yuco (Manihot esculenta Crantz) en el trópico. Ph.D. Dissertation. UniversidadNacional de Colombia, Palmira, Colombia, p. 122.

Monsi, M., Saeki, T., 2005. On the factor of light in plant communities and its importance for matter production. Ann. Bot. 95 (3), 549–567. https://doi.org/10.1093/aob/mci052.

NASA Langley Research Center, 2022. NASA POWER: Prediction Of Worldwide Energy Resources. ⟨https://power.larc.nasa.gov/⟩ (Accessed 10 January 2022).

Ospina, B., Jiménez, A., Lopez, V., Pantoja, A., Prakash, A., Taguchi, M., Gómez, H., García, A., 2016. A Look at the Potential of the Crop to Promote Agricultural Development and Economic Growth: Cassava in the Caribbean region. FAO, CLAYUCA and IICA, Bridgetown, Barbados (Accessed 10 January 2022). ⟨https://repositorio.iica.int/handle/11324/2665⟩.

Raes, D., 2009. The ET0 calculator – evapotranspiration from a reference surface. Reference Manual, Version 3.1. FAO, Land and Water Digital Media Series No. 36, Rome, Italy. p. 38. ⟨https://www.fao.org/land-water/databases-and-software/eto-calculator/en/⟩ (Accessed 10 January 2022).

Raes, D., Steduto, P., Hsiao, T.C., Fereres, E., 2009. AquaCrop: the FAO crop model to simulate yield response to water. II. Main algorithms and software description. Agron. J. 101 (3), 438–447. https://doi.org/10.2134/agronj2008.0140s.

Raes, D., 2017a. Understanding AquaCrop. AquaCrop Training Handbooks. FAO,, Rome, Italy, p. 59. ⟨https://www.fao.org/aquacrop/resources/traininghandbooks/en/⟩ (Accessed 10 January 2022).

Raes, D., 2017b. Running AquaCrop. AquaCrop Training Handbooks. FAO, Rome, Italy, p. 117. ⟨https://www.fao.org/aquacrop/resources/traininghandbooks/en/⟩ (Accessed 10 January 2022).

Saxton, K.E., Rawls, W.J., 2006. Soil water characteristic estimates by texture and organic matter for hydrologic solutions. Soil Sci. Soc. Am. J. 70 (5), 1569–1578. https://doi.org/10.2136/sssaj2005.0117.

Selvaraj, M.G., Valderrama, M., Guzman, D., Valencia, M., Ruiz, H., Acharjee, A., 2020. Machine learning for high-through-put field phenotyping and image processing provides insight in to the association of above and below-ground traits in cassava (*Manihot esculenta* Crantz). Plant Methods 16 (87), 19. https://doi.org/10.1186/s13007-020-00625-1.

Steduto, P., 2003. Biomass Water Productivity: Comparing the Growth-Engines for Crop Models. FAO Expert Consultation on Crop Water Productivity Under Deficient Water Supply, 26–28 February 2003, Rome, Italy.

Steduto, P., Hsiao, T.C., Fereres, E., 2007. On the conservative behavior of biomass water productivity. Irrig. Sci. 25, 189–207. https://doi.org/10.1007/s00271-007-0064-1.

Steduto, P., Hsiao, T.C., Raes, D., Fereres, E., 2009. AquaCrop: The FAO crop model to simulate yield response to water. I. Concepts and underlying principles. Agron. J. 101 (3), 426–437. https://doi.org/10.2134/agronj2008.0139s.

Steduto, P., Hsiao, T.C., Fereres, E., Raes, D., 2012. Crop Yield Response to Water. FAO Irrigation and Drainage Paper 66. FAO, Rome, Italy, p. 505. ⟨https://www.fao.org/3/i2800e/i2800e00.htm⟩ (Accessed 10 January 2022).

Van Der Zaag, D.E., 1984. Reliability and significance of a simple method of estimating the potential yield of the potato crop. Potato Res. 27 (1), 51–73. https://doi.org/10.1007/bf02356197.

Veltkamp, H.J., 1985. Physiological Causes of Yield Variation in Cassava (Manihot esculenta Crantz). Ph.D. Dissertation. Wageningen University, Netherlands, p. 132. ⟨https://edepot.wur.nl/205651⟩.

Wellens, J., Raes, D., Traore, F., Denis, A., Djaby, B., Tychon, B., 2013. Performance assessment of the FAO AquaCrop model for irrigated cabbage on farmer plots in a semi-arid environment. Agr. Water Manag. 127, 40–47. https://doi.org/10.1016/j.agwat.2013.05.012.

Wellens, J., Sall, M.T., Ville, A., 2020. Processing chain for parcel and regional crop monitoring (PROCCY): Open Data, Sentinel-2, AquaCrop and sugar cane. iCROPM 2020 Symposium: Crop Modelling for the Future. 3-5 February 2020, Montpellier, France. Book of abstracts, 165-166.

FAOSTAT, 2021. FAOSTAT Database. FAO, Rome, Italy. http://faostat.fao.org/ (accessed 30 September 2021).